Overcoming the Undesirable CRISPR-Cas9 Expression in Gene Correction

Emily Xia,[1,2] Rongqi Duan,[1] Fushan Shi,[1,4] Kyle E. Seigel,[1,2] Hartmut Grasemann,[1,3] and Jim Hu[1,2,3]

[1]Translational Medicine, Hospital for Sick Children Research Institute, 686 Bay Street, Toronto, ON M5G 0A4, Canada; [2]Department of Laboratory Medicine and Pathobiology, University of Toronto, 1 King's College Circle, Toronto, ON M5S 1A8, Canada; [3]Department of Paediatrics, University of Toronto, 1 King's College Circle, Toronto, ON M5S 1A8, Canada

The CRISPR-Cas9 system is attractive for gene therapy, as it allows for permanent genetic correction. However, as a new technology, Cas9 gene editing in clinical applications faces major challenges, such as safe delivery and gene targeting efficiency. Cas9 is a foreign protein to recipient cells; thus, its expression may prompt the immune system to eliminate gene-edited cells. To overcome these challenges, we have engineered a novel delivery system based on the helper-dependent adenoviral (HD-Ad) vector, which is capable of delivering genes to airway basal stem cells *in vivo*. Using this system, we demonstrate the successful co-delivery of both CRISPR-Cas9/single-guide RNA and the LacZ reporter or *CFTR* gene as donor DNA to cultured cells. HD-Ad vector genome integrity is compromised following donor DNA integration, and because the CRISPR-Cas9/single-guide RNA and donor DNA are carried on the same vector, CRISPR-Cas9 expression is concurrently eliminated. Thus, we show the feasibility of site-specific gene targeting with limited Cas9 expression. In addition, we achieved stable *CFTR* expression and functional correction in cultured cells following successful gene integration.

INTRODUCTION

Cystic fibrosis (CF) is a monogenic disease caused by mutations in the *CFTR* gene and is characterized by progressive lung disease due to impaired mucociliary clearance, chronic airway inflammation, and infection. For genetic diseases such as CF, gene therapy is an attractive therapeutic approach, as it targets the underlying genetic defects that give rise to disease pathology. CF is an ideal candidate for lung gene therapy, as it is a monogenic disease, and the airway epithelium is readily accessible to gene delivery vectors. Accordingly, more than 20 CF gene therapy trials have been conducted since the 1990s.[1–6] Despite advancements in vector development[7] and delivery,[8] however, major challenges remain. First, the airway immune response represents a significant barrier to stable transgene expression, as the lung is an immune-sensitive organ.[9,10] Furthermore, repeated vector administration is required when targeting the airway epithelium due to epithelial cell turnover. The host adaptive immune response makes this an ineffective strategy, as evidenced by previous clinical trials. These limitations could be overcome by permanently correcting a mutated *CFTR* gene in airway stem cells, the source of airway epithelial renewal.

New technologies for targeted gene editing, such as CRISPR, can be utilized to overcome the limitations of conventional gene therapy. CRISPR systems are natively involved in bacterial immune defense against viral infection.[11] Of the variety of CRISPR systems, CRISPR-Cas9 has been extensively engineered and repurposed as a versatile gene editing tool for use in cells[12–14] and animal models.[15–19] Cas9 is co-expressed with a programmable single-guide RNA (sgRNA) that guides Cas9 to induce a site-specific double-strand break (DSB) at a predetermined genomic locus. Gene knock-outs can be generated when the cell uses non-homologous end joining (NHEJ) to repair the DSB. In contrast, homology-directed repair (HDR) can be exploited to integrate therapeutic genes, such as *CFTR*, into a precise genomic locus. The latter mechanism could, therefore, be harnessed to permanently correct the *CFTR* genetic defect in CF patients. This approach ultimately requires an efficient gene therapy vector that can co-deliver Cas9-sgRNA and the *CFTR* gene to target cells.

Both viral and liposomal vectors are conventionally used to deliver genes *in vivo*.[8] Commonly used viral vectors are based on adenoviruses, adeno-associated viruses (AAVs), lentiviruses, and retroviruses.[4] Notably, AAV vectors have been clinically successful in treating the retinal degenerative disease Leber congenital amaurosis (LCA),[20–22] as well as lipoprotein lipase deficiency.[23] More recently, Cas9 has been delivered in AAV vectors to correct mutations in the dystrophin gene in mouse models of Duchenne muscular dystrophy (DMD).[24,25] However, donor DNA is not required in the case of DMD due to the particular nature of the genetic defect, and the limited AAV DNA carrying capacity of 4.7 kb is, therefore, sufficient for this application. In contrast, for applications requiring both Cas9 and large therapeutic genes, a vector with an expanded carrying capacity is required.

Helper-dependent adenoviral (HD-Ad) vectors are based on adenovirus serotype 5 with all viral coding sequences deleted.[26] This

increases the DNA carrying capacity to ∼37 kb and reduces vector immunogenicity. Furthermore, these vectors maintain the natural adenovirus tropism for epithelial transduction, a favorable asset for airway gene delivery. In fact, our group has recently demonstrated that HD-Ad vectors can transduce airway basal cells[27]—which harbor stem cell-like properties—of mice and pigs *in vivo*, as well as human primary cells. These vectors may, therefore, be ideal gene delivery vehicles for the co-delivery of Cas9-sgRNA and large therapeutic genes such as *CFTR*.

Here, we produced HD-Ad vectors containing both Cas9-sgRNA and donor DNA designed to integrate reporter genes or *CFTR* into the AAVS1 genomic locus in human cells. We demonstrate successful site-specific *CFTR* gene integration resulting in vector-specific *CFTR* protein expression. Successfully integrating the wild-type *CFTR* gene consequently rescued *CFTR* channel activity in a CF cell line. Interestingly, we also found that, following successful gene integration, CRISPR-containing HD-Ad vectors are rapidly degraded in transduced cells. The degradation of vector genomes effectively eliminates residual Cas9 expression in transduced cells. The elimination of Cas9 expression would presumably reduce immunogenicity and off-target edits, which is therapeutically desirable for CRISPR-based gene therapies. Accordingly, we have termed this approach "scarless gene correction." Taken together, we demonstrate the feasibility of using HD-Ad vectors for the stable integration of the *CFTR* gene, which may ultimately aid in developing a safe model for CRISPR-Cas9 CF gene therapy.

RESULTS

Co-expression of Cas9 and Donor DNA from a Single HD-Ad Vector

In order to assess the feasibility of packaging Cas9-sgRNA and therapeutic donor DNA into a single HD-Ad vector, we first generated a vector with the LacZ reporter gene as donor DNA. This HD-Ad vector contains an expression cassette for Cas9 and an sgRNA targeting exon 2 of the AAVS1 locus, which is regarded as a safe harbor for genomic integration and is ubiquitously expressed in a variety of cell types. The donor DNA is a LacZ expression cassette flanked on either side by homology arms of various lengths, ranging from 1 to 4 kb, which are homologous to the AAVS1 locus on either side of the Cas9 cutting site (Figures 1A and 1C; Table 1). HD-Ad vectors were produced as described previously.[28] Cas9 was tagged with GFP to assess transduction efficiency, which was close to 100% at a vector concentration of 100 MOI (infectious particles per cell) (Figure 1D). These data were confirmed by X-gal staining in IB3-1 cells transduced at 50, 100, and 150 MOI (Figure 1D), which all expressed significant levels of Cas9 mRNA, as measured by qPCR (Figure 1E). Co-expression of the LacZ reporter gene with Cas9 in transduced cells was also demonstrated by staining cells with a fluorescent substrate, ImaGene Red (Figure S1). Cas9 cleavage efficiencies in cells transduced at 100 and 150 MOI were 53.5% and 60.0% for HEK293 cells, 62.3% and 82.3% for IB3-1 cells, and 43.1% and 67.6% for A549 cells, respectively (Figure 1B; Figure S2). These results indicate that HD-Ad vectors can co-deliver Cas9-sgRNA and large donor DNA cassettes to

cultured human cell lines and achieve efficient chromosomal cleavage at the targeted locus.

### HD-Ad Vectors Mediate Gene Integration at Targeted Locus

To evaluate whether HD-Ad vectors can mediate site-specific gene integration, PCR primers were designed to amplify the junction site between the integrated cassette and the targeted genomic locus (Figures 2A and 2B). Junction PCR was performed at 2-day intervals between 3 and 11 days post-transduction for three reporter vectors in IB3-1 cells. An HD-Ad LacZ vector that lacks the Cas9 gene was used as a negative control. For all three reporter vectors, junction PCR showed positive band products at the predicted sizes (Figures 2A and 2B; Figure S3). PCR products were then purified and digested with restriction enzymes to verify their identity. Sanger sequencing was used to locate the precise junction of integration (Figures 2A and 2B; Figure S3). Furthermore, junction PCR was performed on the top 3 predicted off-target loci based on *in silico* predictions from http://crispr.mit.edu,[29] in order to assess potential off-target integration events. Junction PCR using primers flanking off-target loci did not yield PCR products (Figure S4), indicating that reporter virus integration events were restricted to the desired chromosomal locus.

Transient Expression of Cas9 from HD-Ad Vectors

The HD-Ad vector genome has been shown to remain stable in the episomal compartment in transduced cells.[30] However, GFP fluorescence evidently decreased at a faster rate from HD-Ad vectors expressing Cas9 (K18-1-1), compared to control vectors expressing GFP in IB3-1 cells (Figure 3A; Figure S5). Therefore, we measured the amount of residual vector genome by qPCR at various time points post-transduction and observed an accelerated loss of HD-Ad CRISPR genomes as compared to control vectors not expressing Cas9 (Figure S6). These results were supported by qPCR and western blot analysis, showing fast decline in both Cas9 mRNA and protein expression in cells transduced with K18-1-1 vector (Figures 3B, 3C, and 3F; Figure S7). By day 7, virtually no vector genomes were detectable (Figure 3D).

To quantify the levels of residual Cas9 expression in cells with positive integrations, colonies derived from integrated single cells were selected for further analysis. qPCR of Cas9 mRNA from these colonies revealed no Cas9 expression (Cas9 mRNA from day 3), while LacZ mRNA was abundant (Figures 3E and 3F). In addition, these integrated cell colonies had no apparent viral genome present (Figure 3F). These results collectively suggest that following vector transduction and gene integration, the vector genome and Cas9 expression were consequently lost.

A possible explanation for this phenomenon is that expression of Cas9 may have caused cell apoptosis. To examine this, we performed flow cytometry on annexin V and 7AAD double-stained cells transduced with HD-Ad CRISPR vectors (Figure 4). Results demonstrated that neither HD-Ad control vectors nor Cas9-expressing HD-Ad vectors caused significant cellular apoptosis. This experiment also
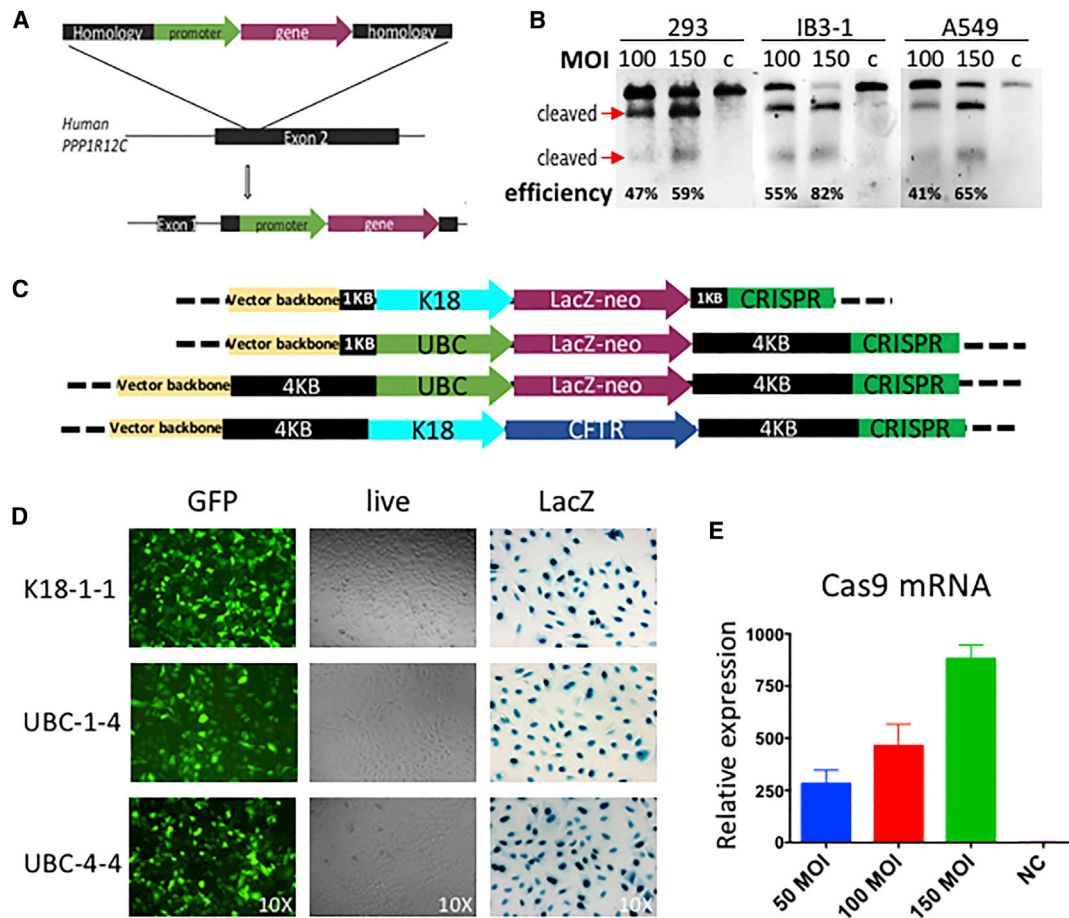
Figure 1. Co-delivery of CRISPR-Cas9 System and Donor Genes to Target the AAVS1 Locus Using HD-Ad Vectors

(A) Gene targeting strategy. A donor gene with its own promoter flanked by homology arms targets exon 2 of the human AAVSI locus or PPP1R12C gene, resulting in integration of the donor gene with its promoter. (B) T7E1 assays for measuring CRISPR-Cas9 cleavage efficiency. HEK293, IB3-1, and A549 cells were transduced with UBC-4-4 HD-Ad vector at 100 MOI or 150 MOI. Total cellular genomic DNA was isolated 3 days post-transduction. T7E1 assays were performed. c indicates the result from cells transduced with a control HD-Ad vector, C4HSU, which does not contain Cas9. (C) Schematic diagram of the genomes of HD-Ad vectors for co-delivery of the CRISPR system and donor genes. Three reporters and a *CFTR* vector genome are illustrated. K18-1-1, LacZ reporter gene under the control of the K18 promoter flanked by 1-kb homology arms; UBC-1-4, LacZ reporter vector with a 1-kb homology arm on the left side and a 4-kb homology arm on the right side, and the reporter gene is driven by the human ubiquitin C (UBC) gene promoter; UBC-4-4, LacZ reporter vector with a 4-kb homology arm on each side, and the reporter gene is driven by the UBC promoter; and CFTR-4-4, *CFTR* vector with a 4-kb homology arm on either side, and *CFTR* expression is driven by the K18 promoter. Each viral construct also contains the Cas9 gene and a guide RNA gene that targets the AAVSI locus as well as viral backbone components that are necessary for viral packaging and production. (D) EGFP and LacZ expression from reporter HD-Ad vectors. EGFP signal indicates Cas9 expression, since both are translated from the same mRNA. LacZ gene expression was detected via X-gal staining. Transduction using 100-MOI viruses resulted in robust LacZ gene expression in human A549 cells. (E) Expression of Cas9 mRNA 72 hr post-transduction with different viral dosages. Total RNA was prepared from the transduced cells, and qRT-PCR was performed to assess the level of Cas9 mRNA expression. The y axis represents relative gene expression in comparison to negative control of each individual experiment. NC, negative control.

indicates that our vector system does not induce cell death as a consequence of targeted gene integration.

Efficiency of Reporter Gene Integration

We used HD-Ad LacZ vectors with different homology arm lengths to examine the effect of arm lengths on integration efficiency (Figure 1B). The efficiency of integration was examined by two different approaches. First, the transduced cells were subjected to X-gal staining following 10 culture passages (Figure 5A). We also sorted and cultured the transduced cells in 96-well plates, followed by X-gal staining (Figure 5B). These experiments indicated that homology arm length does indeed influence gene integration efficiency, and the longest homology arms (4 kb) were associated with the highest efficiencies of 8%–10% (Figures 5A and 5B). Homology arm length is, therefore, an important factor for the integration efficiency of large genes (the LacZ gene cassette is ~8 kb). We also investigated the influence of the small molecule SCR7, a NHEJ inhibitor that has been extensively used to enhance CRISPR-mediated integration

Table 1. Name and Description of Integration Vectors Used

HD-Ad Vector Name	CRIPSR- Cas9	Vector Backbone	Donor Gene	Donor Gene Promoter	Homology Arm Length (L/R)	GFP
K18-1-1	Y	PC4SHU	lacZ	K18	1 kb/1 kb	Y
UBC-1-4	Y	PC4SHU	LacZ	UBC	1 kb/4 kb	Y
UBC-4-4	Y	PC4SHU	lacZ	UBC	4 kb/4 kb	Y
CFTR-4-4	Y	PC4SHU	CFTR	K18	4 kb/4 kb	Y
K18-lacZ	N	PC4SHU	lacZ[a]	K18	0 kb/0 kb[b]	N
CMV-GFP	N	PC4SHU	GFP[a]	CMV	0 kb/0 kb[b]	Y

L/R, left/right; Y, yes; N, no.[a]Not used as donor.
[b]Control vectors without donor homology arms.

efficiency.[31] Our results show that for HD-Ad vectors, SCR7 can further enhance the efficiency of integration by ∼1.5-fold (Figure 5B; Figure S8).

Integration of *CFTR* Using HD-Ad Vectors

Since our ultimate goal is to develop gene therapy strategies for CF, we designed an HD-Ad vector to integrate the *CFTR* gene into the AAVS1 locus. For this purpose, we utilized a *CFTR* gene cassette flanked on both sides by 4-kb homology arms. Junction PCR showed precise integration within AAVS1 (Figure 6A). Furthermore, *CFTR* mRNA and protein expression were assessed immediately after vector transduction and after 6–12 passages. Passaging cultured cells dilutes non-integrated vectors and, therefore, increases the relative contribution of *CFTR* expression from the integrated *CFTR* gene. Results indicated that, after passaging cells, a significant amount of *CFTR* expression remained, as determined by qPCR and western blotting. Therefore, HD-Ad vectors are capable of integrating *CFTR* into the AAVS1 locus with an efficiency that results in considerable long-term *CFTR* expression (Figure 6B). To assess functional correction, we measured *CFTR* channel function using the iodide efflux assay following *CFTR* gene integration in a CF cell line (IB3-1).[32] Human IB3-1 cells transduced with either HD-Ad-CRISPR-CFTR or a control vector without CRISPR were passaged 12 times to dilute out residual vector. Results showed that cells treated with HD-Ad-CRISPR-CFTR had measurable *CFTR* channel function, whereas cells transduced with control vector failed to show *CFTR* channel activity (Figure 6C).

DISCUSSION

In this study, we demonstrate that HD-Ad vectors can be used to co-deliver Cas9-sgRNA and large donor DNA to achieve site-specific gene integration in cultured human cells. There are several advantages in using this vector system for CRISPR-mediated gene targeting in airway epithelium. Since HD-Ad vectors are able to deliver both donor DNA and Cas9-sgRNA simultaneously, this approach will be more efficient than vector systems that require two vectors for delivery. The extended carrying capacity not only facilitates the delivery of large genes such as *CFTR* but also allows for the co-delivery of additional factors with the potential to further enhance gene targeting efficiency. Furthermore, our delivery system can achieve site-specific

therapeutic gene integration and simultaneous destruction of residual vector genome. This will avoid long-term Cas9 expression, which may exacerbate the host immune response in clinical applications. The HD-Ad vector delivery system can, therefore, achieve scarless therapeutic gene integration.

We observed a rapid decline in Cas9 expression and vector genomes following cell transduction (Figure 3). This is evidently not a consequence of Cas9-induced apoptosis, as demonstrated by flow cytometry analysis (Figure 4). This phenomenon could potentially be caused by different factors. First, vector genomes are expected to be diluted as a result of cell division, since the vector genome does not replicate in transduced cells. This would also be true for the control vector. Second, following donor DNA integration, the integrity of the vector genome is compromised, which is expected to lead to vector genome destruction. Currently, it is unknown whether there are any other factors that could cause vector destruction.

We have also examined factors that may influence gene integration efficiency, such as homology arm length. We found that the efficiency of reporter gene integration can be enhanced by extending homology arm length, as the vector with 4-kb homology arms yielded higher integration efficiencies than vectors with shorter homology arms (Figure 5). Gene integration efficiency can also be enhanced by inhibiting the NHEJ pathway. SCR7 has been widely reported in the literature to enhance gene integration efficiency up to severalfold.[31] In this study, we found that SCR7 enhanced the efficiency of integration by 1.5-fold.

The junction PCR assays demonstrate that our CRISPR-mediated gene integration strategy can successfully target the AAVS1 genomic safe harbor. One limitation in our analysis of target specificity is that we could not provide data on potential non-specific, non-CRISPR-mediated gene integration. Theoretically, this could take place by either whole vector integration or partial vector integration. Whole vector integration is unlikely, however, as we failed to detect GFP expression from our vectors after passaging transduced cells more than 10 times. It is difficult to determine whether there is any partial vector non-specifically integrated and where such non-specific integration may occur. CRISPR specificity was not a major focus of this work. However, clinical studies will likely
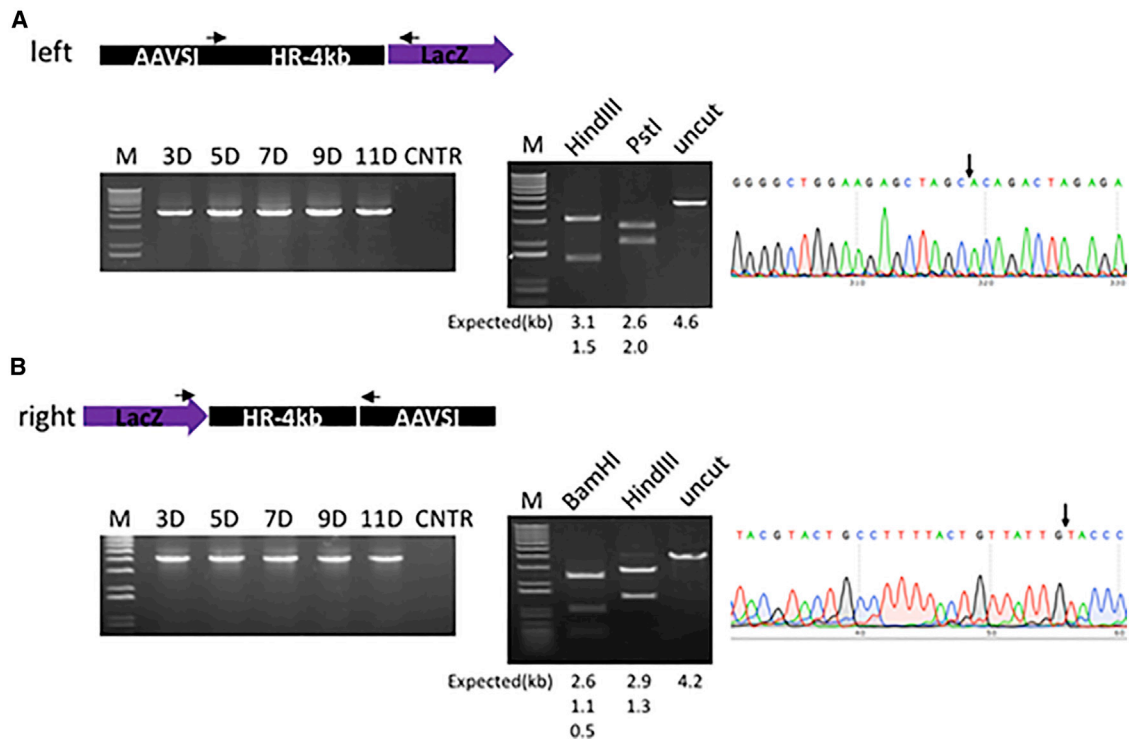
Figure 2. Determination of the Gene Integration Site by Junctional PCR

(A) PCR analysis of the integration site of the left homology arm. Primers were designed with one binding upstream of the integration site and the other binding within the promoter region of the donor LacZ gene. PCR was performed with genomic DNA isolated from cells at days 3, 5, 7, 9, and 11 post-transduction. CNTR indicates PCR result from cells transduced with a control K18-LacZ vector that did not contain the Cas9 gene. PCR products were further purified and analyzed by restriction digestion using HindIII and PstI and by Sanger sequencing analysis. (B) PCR analysis of the integration site of the right homology arm. The analysis was performed as described in (A).

use specificity-improved Cas9 variants,[33,34] and we will leave this as a topic for future studies.

Using junction PCR analyses, we have also shown that a *CFTR* gene expression cassette can be integrated into the AAVS1 locus, which was confirmed with DNA sequencing (Figure 6). It is evident that successful integration of this cassette leads to stable *CFTR* mRNA and protein expression, as well as functional correction of *CFTR* ion channel activity in a CF cell line (Figure 6C). These results collectively demonstrate that *CFTR* channel activity can be rescued by CRISPR-mediated integration of *CFTR* gene cassettes through HD-Ad vector delivery.

In summary, this study provides proof of concept that HD-Ad vectors can be used to successfully deliver gene editing tools to site-specifically integrate therapeutic genes without leaving undesirable genetic material behind. Thus, our approach can be used in gene editing studies where delivery is more difficult, such as in primary epithelial cells. More importantly, our vector system avoids long-term expression of vector-related foreign antigens, such as CRISPR-Cas9, in gene-targeted cells. This approach, therefore, minimizes immunogenicity and has great potential for therapeutic *in vivo* applications. This is especially important in light of recent findings regarding the presence of naturally occurring human antibodies against CRISPR.[35]

MATERIALS AND METHODS

HD-Ad Vector Cloning and Production

For cloning of the K18-1-1, UBC-1-4, and UBC-4-4 vectors, the LacZ gene, left and right homology arms, and Cas9 were cloned individually into the pC4HSU vector backbone, which contains a packaging signal, inverted terminal repeats, and stuffer DNA.[36] A 20-nt guide RNA sequence, 5′-ACCCCACAGTGGGGCCACTA-3′, was cloned into Cas9 plasmid (catalog no. PX458; Addgene, Cambridge, MA, USA) BbsI site. For the K18-1-1 vector, the Cas9 gene with guide RNA was placed into the pC4HSU vector's AscI site. The 1kb-K18-LacZ-neo-1kb donor construct was cloned into the SalI site in the pC4HSU backbone. For the UBC-1-4 vector, K18-LacZ-neo-1-4 was inserted into the vector backbone using the XhoI and NotI sites, and Cas9 was inserted into the vector backbone using the NotI and EcoRV sites. For the UBC-4-4 vector, KpnI was used to insert the right 4-kb homology arm, BglII was used to insert the left homology arm, and Cas9 was cloned into the vector using the XhoI and SmaI sites. For the CFTR-4-4 vector, 4-kb left and right arms were inserted into the pU4HSU vector backbone using the NdeI and KpnI sites. K18-CFTR-4-4 was then inserted into the viral vector backbone using
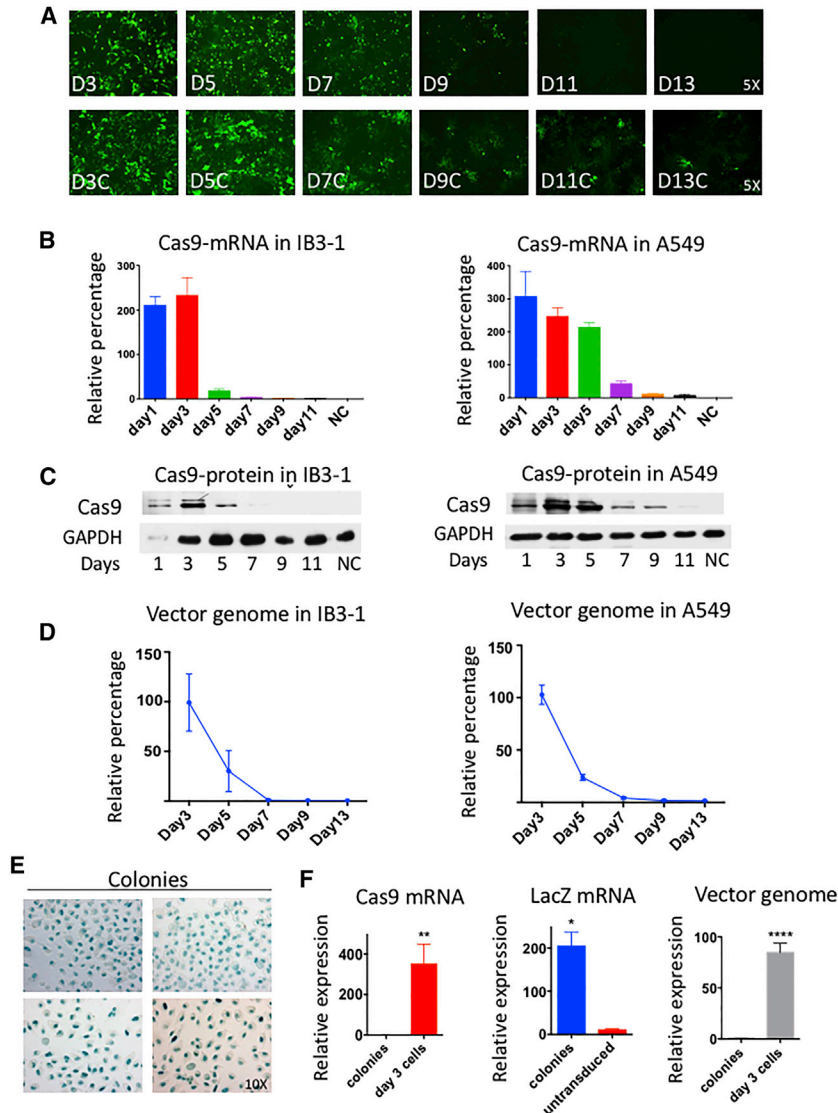
Figure 3. Transient Expression of Cas9 Correlated with the Decline of Vector Genomes in Transduced Cells

(A) Time course of EGFP expression in IB3-1 cells transduced with the HD-Ad vector (K18-1-1) or CNTR (CMV-GFP) vector at 50 MOI. Fluorescent images were taken at days 3, 5, 7, 11, and 13 post-transduction. (B) qPCR analysis of cas9 mRNA for IB3-1 cells (left) and A549 cells (right) at different time points after K18-1-1 vector transduction. NC, cells transduced with a K18-LacZ vector that did not contain CRISPR-cas9. (C) Cas9 protein level measured at different time points following K18-1-1 vector transduction. (D) Analysis of relative K18-1-1 vector genome quantity compared to that isolated from day-3 cells. Day-3 vector genome was given 100%. Vector genome measurements were made against the packaging signal of the HD-Ad vector in IB3-1 (left) and A549 (right) cells. (E) LacZ images of positively integrated colonies. (F) Left: relative Cas9 mRNA level from positively integrated colonies compared to that from day 3. Positively integrated colonies were isolated from single-cell cultures of UBC-4-4 transduced cells. Middle: relative LacZ mRNA from positively integrated colonies compared to that of non-transduced cells (n = 4). qPCR analysis was performed using the ΔΔCt method. Right: HD-Ad vector genome measurement in positively integrated colonies (n = 4) compared to that of DNA isolated from day 3.

X-gal Staining

For X-gal staining related to integration efficiency analysis, cells were seeded in 6-well plates at low density ($5 \times 10^4 - 1 \times 10^5$ cells per well) and let to proliferate until 80% confluency. This allows easier spotting of positive colonies. Then, cells were washed $2\times$ with PBS (pH 7.8), followed by fixing for 10 min in 0.5% glutaraldehyde dissolved in PBS (pH 7.8). After fixing, cells were washed 2 times with 1 mL PBS (pH 7.8). X-gal staining solution containing 2 mM $MgCl_2$ was made by dissolving 5-bromo-4-chloro-3-indolyl β-D-galac-topyranoside (X-gal) reagent in PBS. Reactions occurred in the dark for 4 hr at 37°C. The cells were washed $3\times$ with PBS and photographed under a microscope.

the XhoI and AsisI sites. Vector production was carried out as described.[37]

Cell Culture and Transduction

Human cell lines, A549[38] and IB3-1,[39] were maintained in DMEM (GIBCO, Waltham, MA, USA) with 10% fetal bovine serum (FBS) and 1% penicillin-streptomycin (Thermo Fisher Scientific, Waltham, MA, USA). Cells were maintained in a tissue culture incubator at 37°C with humidified air, 5% CO_2. Seeding density for transduction experiments were 3×10^5 cells per well for 6-well plates and 1×10^5 cells per well for 12-well plates. Transduction was carried out by mixing cells with vector particles in a serum-free medium of half the original volume for 1 hr, followed by the addition of half the original volume of the medium with 20% FBS. Vector transduction efficiency was monitored by observing reporter gene fluorescence intensity. For cell passaging, one fourth of the original cells were re-plated.

Quantification of Vector Genome and Cas9 mRNA with qPCR

Viral vector genome was quantified with qPCR using primers binding the viral inverted terminal repeat (ITR) region (forward [Fwd]: 5′-CG GTGTACACAGGAAGTGACAA-3′ and reverse [Rev]: 5′-GCGG CCCTAGACAAATATTACG-3′) and total genomic DNA. Genomic DNA was extracted using the DNeasy Blood & Tissue Kit (catalog no. 69504; QIAGEN, Toronto, ON, Canada). Primers against the endogenous GAPDH gene were utilized as an internal control. To calculate the relative viral genome quantity, cycle threshold (Ct) values of internal controls were subtracted from that of the experimental samples to obtain ΔCt of a particular sample. ΔΔCt of each sample was obtained by subtracting the Ct value from that of the negative control. Relative gene expression was calculated using the following formula: relative
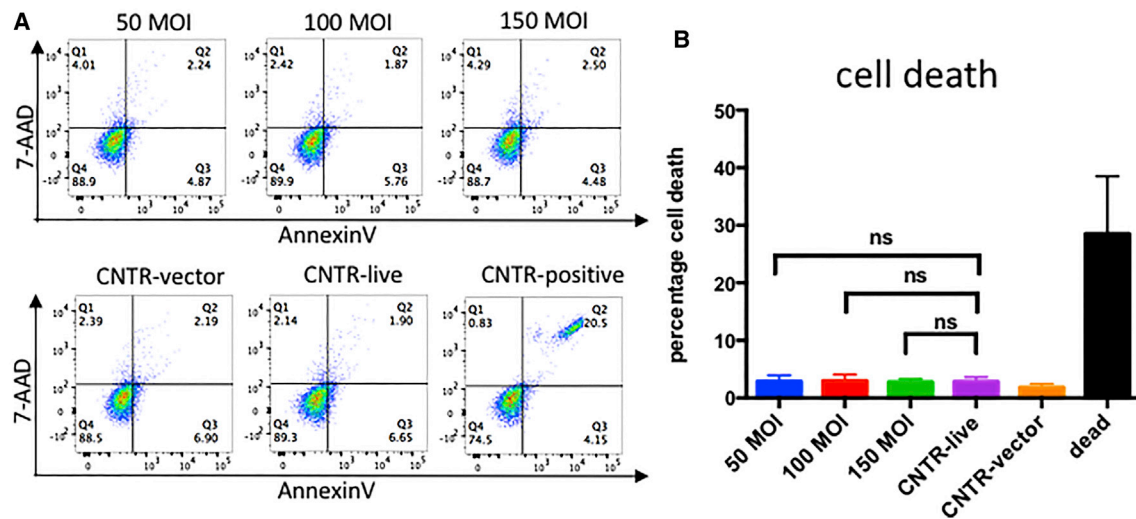
Figure 4. Cell Apoptosis Analysis of IB3-1 Cells Transduced with the HD-Ad Vector UBC-4-4

(A) Plots of flow data from IB3-1 cells transduced with HD-Ad vector (UBC-4-4) at 50, 100, and 150 MOI (top panel). Cell apoptosis was analyzed 72 hr post-transduction using APC-annexin-V and 7-AAD double-staining flow cytometry. Percentages of apoptotic cells were indicated in quadrant 2 (Q2). Three controls are shown in the lower panels. CNTR-vector, IB3-1 cells transduced with K18-LacZ; CNTR-live, live IB3-1 cells with no transduction; CNTR-positive, a mixture of live and heat-killed IB3-1 cells. (B) Bar graph summarizing cell apoptosis results with statistical analysis. ns, p > 0.05, unpaired Student's t test; n = 5.

gene expression = $2^{-\Delta\Delta Ct}$. To measure mRNA levels of Cas9 and LacZ, total RNA from each sample was extracted using the PureLink RNA Mini Kit (catalog no. 12183018A; Thermo Fisher Scientific, Waltham, MA, USA). Reverse transcription from mRNA was performed using the SuperScript VILO Master Mix (catalog no. 11755250; Invitrogen, Waltham, MA, USA). qPCR was performed using a Thermo Fisher Scientific qPCR machine (QuantStudio 3, Applied Biosystems, Waltham, MA, USA) with the Power SYBR Green PCR Master Mix (catalog no. 4368577; Thermo Fisher Scientific, Waltham, MA, USA). Primers against the human GAPDH gene were used as an internal control (Fwd: 5′-GTTCGACAGACAG CCGTGTG-3′; Rev: 5′-ATGGCGAATGTCCACTTTGC-3′).

T7E1 Assay

Total genomic DNA from cells transduced with viral vectors was extracted using a lysis buffer protocol.[40] Briefly, cell lysate was incubated at 55°C for 10 min in combination with proteinase K (10 μL of 10 mg/mL stock). High salt (6 M) NaCl solution was used to precipitate protein from samples. Genomic DNA was precipitated using 650 μL 100% isopropanol. PCR amplification of the target sequence was performed using primer sequences flanking the cleavage site: (Fwd: 5′-CTCAGCTAGTCTTCTTCCTCCAACC-3′ and Rev: 5′-AGGTG AAGAGCCAAAGTTAGAACTCAG-3′). PCR fragments were purified using the Clontech PCR Clean-Up Kit and allowed to hybridize using the following program: 95°C for 5 min; 85–85°C, −2°C/s; 85–25°C, −0.1°C/s; 4°C hold. T7 endonuclease digestion was allowed to proceed at 37°C in a 20-μL volume for 40 min with 1 μL T7 endonuclease enzyme (catalog no. M0302L; New England Biolabs, Whitby, ON, Canada). Products were visualized on a 2% agarose gel. Band intensities were analyzed using ImageJ.

Western Blotting

To assess Cas9 protein expression, total cellular protein was extracted using radioimmunoprecipitation assay (RIPA) buffer containing proteinase cOmplete Mini Protease Inhibitor Cocktail Tablets (catalog no. 11836153001; Sigma, Oakville, ON, CA). Protein concentration in samples was measured using the BCA kit (catalog no. 7780; NEB, Whitby, ON, Canada). Fifty micrograms of protein per sample was mixed with 5× SDS loading buffer, incubated at 95°C for 5 min, and subsequently loaded onto a 6.5% polyacrylamide gel. Gels were allowed to run at 100 V for 1 hr. Proteins were then transferred onto a nitrocellulose membrane (0.45 μm) at 100 V for 80 min. Membranes were incubated in blocking buffer (5%) skim milk for 2 hr at room temperature, followed by incubation in primary antibody (1:800) dilution at 4°C degrees overnight. Membranes were washed 5 times (10 min each time) with 0.1% PBS-Tween-2- (PBS-T) and subsequently incubated with anti-rabbit secondary antibody (1:3,000 dilution) at room temperature for 2 hr. Membranes were then washed 4–5 times (15 min each) in 0.1% PBS-T. Cas9 protein was detected by the ECL reagent (catalog no. GERPN2209; Bio-Rad, Mississauga, ON, Canada).

To assess *CFTR* protein expression, total protein was extracted using RIPA buffer containing proteinase cOmplete Mini Protease Inhibitor Cocktail Tablets. Samples were put on ice for 15–20 min, with occasional vortexing, and then centrifuged at 14,000 rpm for 20 min. The supernatant was collected and incubated with equal volumes of sample buffer (0.25% bromophenol blue, 0.5 M DTT, 50% glycerol, 10% SDS) at room temperature for 10 min. Proteins were separated on a 6.5% polyacrylamide gel, as described earlier. Anti-*CFTR* antibody
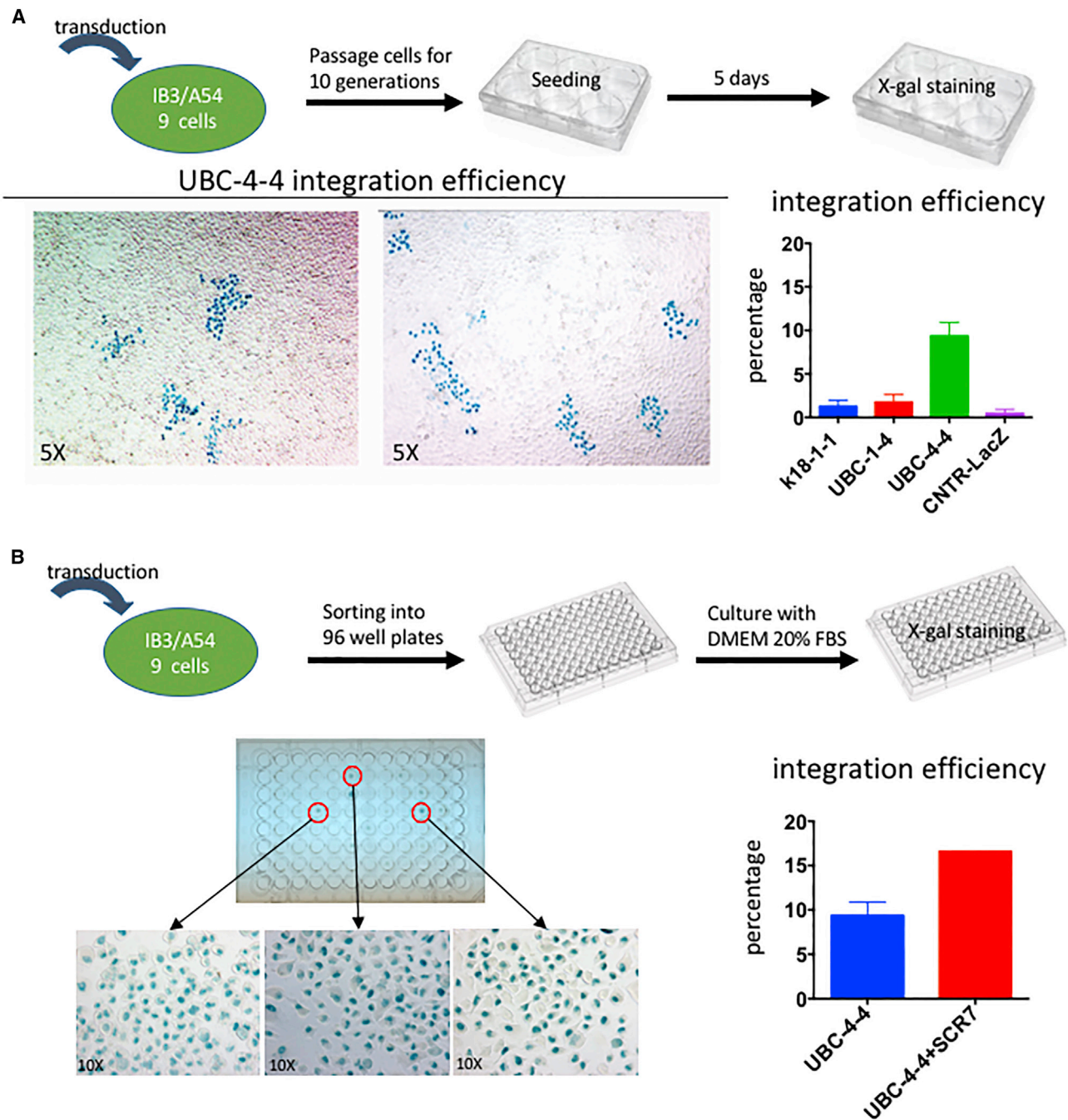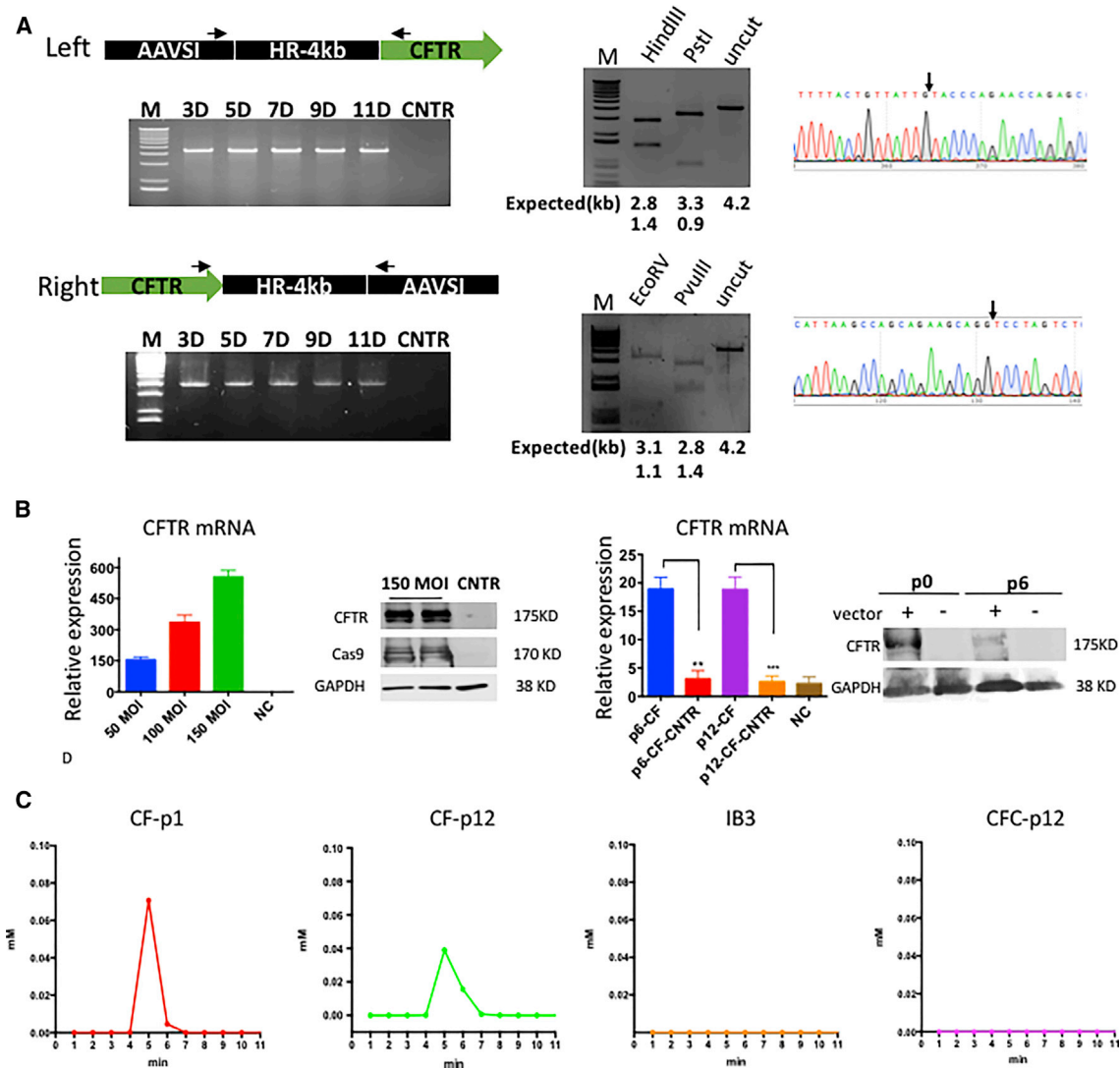
Figure 5. Analysis of CRISPR-Mediated Gene Integration Efficiency

(A) Gene integration assessment via X-gal staining for LacZ-positive cells after consecutive passaging. Cells were cultured and passed for 10 generations and seeded for X-gal staining. CNTR-LacZ, cells transduced with control K18-LacZ vector. (B) Integration assessment via single-cell sorting. IB3-1 cells transduced with UBC-4-4 vector or CNTR vector (K18-LacZ) were sorted into 96-well plates and allow to grow until confluency. SCR7 was added to cells 18 hr post-transduction and sorted as described previously.

(catalog no. MAB1660; R&D Systems, Minneapolis, MN, USA) was used at a concentration of 1:800. Five washes in 0.1% TBS-T (15 min each time) were included between primary and secondary antibody incubation and after secondary antibody incubation. The ECL reagent (catalog no. GERPN2209; Bio-Rad, Mississauga, ON, Canada) was used for signal detection.

Figure 6. Targeting Human *CFTR* Expression to the AAVS1 Locus

(A) Junction PCR analysis of CRISPR-mediated *CFTR* integration. PCR analysis was performed using genomic DNA from IB3-1 cells transduced with 100 MOI of CFTR-4-4 vector at days 3, 5, 7, 9, and 11 post-transduction with primers specific for detection of the left (top) and right (bottom) side homology arm junction. The PCR products were further analyzed by restriction digestion and Sanger sequencing. CNTR represents PCR result from IB3-1 cells transduced with K18-LacZ control vector. (B) Analysis of *CFTR* expression at the mRNA and protein levels. IB3-1 cells were transduced with HD-Ad vector (CFTR 4-4), and levels of *CFTR* mRNA and protein were determined by qRT-PCR and western blotting, respectively. The left panels show mRNA and protein levels in cells 3 days post-transduction. The right panels show the expression levels in transduced cells at passages 6 and 12 (n = 3). (C) Iodide efflux assay of *CFTR* channel function. Vector-transduced IB3-1 cells were loaded with iodide. After washing the cells, a time course of forskolin-stimulated iodide release into the medium was recorded. CF-p1, IB3-1 cells transduced with CFTR-4-4 vector and cultured for 3 days; CF-p12, cells transduced with CFTR-4-4 vector and cultured for 12 passages; IB3, IB3-1 cells with no transduction; CFC-p12, IB3-1 cells transduced with a control *CFTR* vector that does not contain CRISPR-cas9 and passed for 12 generations.

Flow Cytometry

To assess cell apoptosis, transduced cells were trypsinized 3 days post-transduction and washed with cold PBS. The cells were stained with 7-AAD and annexin-V (BD Biosciences, San Jose, CA, USA) and filtered through nylon mesh before flow cytometry analysis (LSRII-CFI BGRV; BD Biosciences, San Jose, CA, USA). Cells were gated from the forward scatter-area (FSC-A), side scatter-area (SSC-A) plot, and subsequently, doublet cells were excluded from analysis from the forward scatter-height (FSC-H), forward scatter-width (FSC-W) plot. Mixed heat-killed and live cells were used as a positive control. Cell killing was carried out by heating cells at 70°C for 5 min. Flow cytometry analysis was performed using FlowJo v10 (Ashland, OR, USA). The p1 gate was set using the FSC-A versus SSC-A plot, the p2 gate for single-cell isolation was set using the FSC-H versus

FSC-W plot, and the p3 gate was set using the 7-AAD versus APC-A plot.

Gene Integration Assessment

The efficiency of integration was evaluated via two different methods. The first method was to count the percentage of the LacZ-positive cells after culturing the transduced cells for 10 passages to dilute out non-integrated vector genomes. The transduced cells were passed every 3 days starting at day 8 post-transduction. Integration efficiency was calculated based on the percentage of X-gal-positive cells at day 30. At this time point, the contribution of non-integrated vector to X-gal-positive cells was expected to be negligible, if there was any. This was consistent with the observation that there were no GFP-positive cells at this time.

The second method was performing single-cell sorting in 96-well plates and counting the reporter-expressing colonies. Transduced cells were trypsinized, washed twice with $1\times$ PBS, and passed through nylon mesh filter before sorting into 96-well plates with 1 cell per well (MoFlo XDP BRV/UV sorter; Beckman Coulter, Indianapolis, IN, USA). Plates were coated with collagen (Advanced BioMatrix, Carlsbad, CA, USA). Cell viability marker (7-AAD) was added to cells to identify viable cell population. The single cells in 96-well plates were subsequently cultured until confluency using DMEM containing 20% FBS. Colonies were stained with X-gal reagent to identify positively integrated colonies or passed for further analyses. To assess the effect of SCR7 on gene targeting efficiency, transduced cells were treated with SCR7 (2 μM) re-suspended in DMSO 18 hr post-transduction. Integration efficiency was evaluated with X-gal staining.

Characterization of Site-Specific Gene Integration

To confirm CRISPR-mediated gene integration into the right chromosomal location, junction PCR experiments were performed, with one primer targeting the sequence's outside the homology arms region at AAVSI, and the other primer binding within the donor gene. Homology arms are as follows: K18-1-1, left side, Fwd: 5′-CTTTGCCACCCTATGCTGA-3′ and Rev: 5′-GCCTGAGCCTG GATTGTT-3′; K18-1-1, right side, Fwd: 5′-GAAGCTCCTCTGT GTCCTCATAAA-3′ and Rev: 5′-GAGAAGGATGCAGGSCGA GAAA-3′; UBC-1-4, left side, Fwd: 5′-TTCAACTGGCCCTGGG CTTA-3′ and Rev: 5′-GGATTCCAGAACTGTCAAGTTGGG-3′; UBC-4-4, right side, Fwd: 5′-CACAGACCGCTTTCTAAGGGT AA-3′ and Rev: 5′-AGTGACCAACCATCCCTGTTT-3′; UBC-4-4, left side, Fwd: 5′-GCTTGGGTTTGCACCAATGATA-3′ and Rev: 5′-CTGTTCCGCTCTCTGGAAAGAA-3′; UBC-4-4, right side, Fwd: 5′- CACAGACCGCTTTCTAAGGGTAA-3′ and Rev: 5′-AGT GACCAACCATCCCTGTTT-3′). Reactions were run for 35–40 cycles. Agarose gel electrophoresis was used to detect the presence of junction PCR products. Gel pictures were taken using the Gel Doc XR+ System (Bio-Rad, Missisauga, ON, Canada). PCR products were further confirmed with restriction analysis and Sanger sequencing performed at the Center for Applied Genomics at the Hospital for Sick Children, Canada.

Iodide Efflux Assay

IB3-1 cells transduced with the *CFTR* integration vector or control vector expressing *CFTR* without CRISPR were passaged 12 generations to dilute out the presence of original vector genomes. Cells were seeded in 6-well plates and incubated in iodide loading buffer (135 mM NaI, 4 mM KNO$_3$, 2 mM Ca(NO$_3$) · 4H$_2$O, 2 mM Mg(NO$_3$) · 6H$_2$O, 11 mM glucose, 20 mM HEPES) for 1 hr. Then, iodide efflux buffer (136 mM NaNO$_3$, 4 mM KNO$_3$, 2 mM Mg(NO$_3$) · 6H$_2$O, 11 mM glucose, 20 mM HEPES) was used to wash cells 8 times (1 mL each time). Efflux buffer containing 20 μM forskolin (catalog no. F6886; Sigma, Oakville, ON, Canada), 0.5 mM 3-isobutyl-1 methyl-xanthine (IBMX), and 0.5 mM cyclic AMP (cAMP) were added to each well and collected at 1-min intervals up to 12 times. The buffer was collected and placed in 24-well plates, and iodide concentration was measured for each sample using an iodide-sensitive electrode (catalog no. 9453BN; Orion, Waltham, MA, USA).

Statistics

Statistical analyses of data were performed with an unpaired Student's t test using Prism. Error bars represent ±SEM. The p values < 0.05 were considered as statistically significant.

SUPPLEMENTAL INFORMATION

Supplemental Information includes eight figures and can be found with this article online at https://doi.org/10.1016/j.omtn.2018.10.015.

AUTHOR CONTRIBUTIONS

ACKNOWLEDGMENTS

REFERENCES

1. Zabner, J., Couture, L.A., Gregory, R.J., Graham, S.M., Smith, A.E., and Welsh, M.J. (1993). Adenovirus-mediated gene transfer transiently corrects the chloride transport defect in nasal epithelia of patients with cystic fibrosis. Cell 75, 207–216.

2. Crystal, R.G., McElvaney, N.G., Rosenfeld, M.A., Chu, C.S., Mastrangeli, A., Hay, J.G., Brody, S.L., Jaffe, H.A., Eissa, N.T., and Danel, C. (1994). Administration of an adenovirus containing the human CFTR cDNA to the respiratory tract of individuals with cystic fibrosis. Nat. Genet. 8, 42–51.

3. Knowles, M.R., Hohneker, K.W., Zhou, Z., Olsen, J.C., Noah, T.L., Hu, P.C., Leigh, M.W., Engelhardt, J.F., Edwards, L.J., Jones, K.R., et al. (1995). A controlled study of adenoviral-vector-mediated gene transfer in the nasal epithelium of patients with cystic fibrosis. N. Engl. J. Med. 333, 823–831.

4. Wagner, J.A., Reynolds, T., Moran, M.L., Moss, R.B., Wine, J.J., Flotte, T.R., and Gardner, P. (1998). Efficient and persistent gene transfer of AAV-CFTR in maxillary sinus. Lancet 351, 1702–1703.

5. Joseph, P.M., O'Sullivan, B.P., Lapey, A., Dorkin, H., Oren, J., Balfour, R., Perricone, M.A., Rosenberg, M., Wadsworth, S.C., Smith, A.E., et al. (2001). Aerosol and lobar administration of a recombinant adenovirus to individuals with cystic fibrosis. I. Methods, safety, and clinical implications. Hum. Gene Ther. *12*, 1369–1382.

6. Perricone, M.A., Morris, J.E., Pavelka, K., Plog, M.S., O'Sullivan, B.P., Joseph, P.M., Dorkin, H., Lapey, A., Balfour, R., Meeker, D.P., et al. (2001). Aerosol and lobar administration of a recombinant adenovirus to individuals with cystic fibrosis. II. Transfection efficiency in airway epithelium. Hum. Gene Ther. *12*, 1383–1394.

7. Cao, H., Koehler, D.R., and Hu, D.J. (2004). Adenoviral vectors for gene replacement therapy. Viral Immunol. *17*, 327–333.

8. Xia, E., Munegowda, M.A., Cao, H., and Hu, J. (2014). Lung gene therapy—How to capture illumination from the light already present in the tunnel. Genes Dis. *1*, 40–52.

9. Hiemstra, P.S. (2007). Antimicrobial peptides in the real world: implications for cystic fibrosis. Eur. Respir. J. *29*, 617–618.

10. Bienenstock, J. (1984). The mucosal immunologic network. Ann. Allergy *53*, 535–540.

11. Makarova, K.S., Grishin, N.V., Shabalina, S.A., Wolf, Y.I., and Koonin, E.V. (2006). A putative RNA-interference-based immune system in prokaryotes: computational analysis of the predicted enzymatic machinery, functional analogies with eukaryotic RNAi, and hypothetical mechanisms of action. Biol. Direct *1*, 7.

12. Kim, J.M., Kim, D., Kim, S., and Kim, J.S. (2014). Genotyping with CRISPR-Cas-derived RNA-guided endonucleases. Nat. Commun. *5*, 3157.

13. Rong, Z., Zhu, S., Xu, Y., and Fu, X. (2014). Homologous recombination in human embryonic stem cells using CRISPR/Cas9 nickase and a long DNA donor template. Protein Cell *5*, 258–260.

14. Kearns, N.A., Genga, R.M.J., Enuameh, M.S., Garber, M., Wolfe, S.A., and Maehr, R. (2014). Cas9 effector-mediated regulation of transcription and differentiation in human pluripotent stem cells. Development *141*, 219–223.

15. Gratz, S.J., Cummings, A.M., Nguyen, J.N., Hamm, D.C., Donohue, L.K., Harrison, M.M., Wildonger, J., and O'Connor-Giles, K.M. (2013). Genome engineering of *Drosophila* with the CRISPR RNA-guided Cas9 nuclease. Genetics *194*, 1029–1035.

16. Chang, N., Sun, C., Gao, L., Zhu, D., Xu, X., Zhu, X., Xiong, J.W., and Xi, J.J. (2013). Genome editing with RNA-guided Cas9 nuclease in zebrafish embryos. Cell Res. *23*, 465–472.

17. Wang, H., Yang, H., Shivalila, C.S., Dawlaty, M.M., Cheng, A.W., Zhang, F., and Jaenisch, R. (2013). One-step generation of mice carrying mutations in multiple genes by CRISPR/Cas-mediated genome engineering. Cell *153*, 910–918.

18. Niu, Y., Shen, B., Cui, Y., Chen, Y., Wang, J., Wang, L., Kang, Y., Zhao, X., Si, W., Li, W., et al. (2014). Generation of gene-modified cynomolgus monkey via Cas9/RNA-mediated gene targeting in one-cell embryos. Cell *156*, 836–843.

19. Hu, X., Chang, N., Wang, X., Zhou, F., Zhou, X., Zhu, X., and Xiong, J.W. (2013). Heritable gene-targeting with gRNA/Cas9 in rats. Cell Res. *23*, 1322–1325.

20. Hauswirth, W.W., Aleman, T.S., Kaushal, S., Cideciyan, A.V., Schwartz, S.B., Wang, L., Conlon, T.J., Boye, S.L., Flotte, T.R., Byrne, B.J., and Jacobson, S.G. (2008). Treatment of Leber congenital amaurosis due to RPE65 mutations by ocular subretinal injection of adeno-associated virus gene vector: short-term results of a phase I trial. Hum. Gene Ther. *19*, 979–990.

21. Simonelli, F., Maguire, A.M., Testa, F., Pierce, E.A., Mingozzi, F., Bennicelli, J.L., Rossi, S., Marshall, K., Banfi, S., Surace, E.M., et al. (2010). Gene therapy for Leber's congenital amaurosis is safe and effective through 1.5 years after vector administration. Mol. Ther. *18*, 643–650.

22. Jacobson, S.G., Cideciyan, A.V., Ratnakaram, R., Heon, E., Schwartz, S.B., Roman, A.J., Peden, M.C., Aleman, T.S., Boye, S.L., Sumaroka, A., et al. (2012). Gene therapy for Leber congenital amaurosis caused by RPE65 mutations: safety and efficacy in 15 children and adults followed up to 3 years. Arch. Ophthalmol. *130*, 9–24.

23. Gaudet, D., Méthot, J., Déry, S., Brisson, D., Essiembre, C., Tremblay, G., Tremblay, K., de Wal, J., Twisk, J., van den Bulk, N., et al. (2013). Efficacy and long-term safety of alipogene tiparvovec (AAV1-LPLS447X) gene therapy for lipoprotein lipase deficiency: an open-label trial. Gene Ther. *20*, 361–369.

24. El Refaey, M., Xu, L., Gao, Y., Canan, B.D., Adesanya, T.M.A., Warner, S.C., Akagi, K., Symer, D.E., Mohler, P.J., Ma, J., et al. (2017). In vivo genome editing restores dystrophin expression and cardiac function in dystrophic mice. Circ. Res. *121*, 923–929.

25. Kemaladewi, D.U., Maino, E., Hyatt, E., Hou, H., Ding, M., Place, K.M., Zhu, X., Bassi, P., Baghestani, Z., Deshwar, A.G., et al. (2017). Correction of a splicing defect in a mouse model of congenital muscular dystrophy type 1A using a homology-directed-repair-independent mechanism. Nat. Med. *23*, 984–989.

26. Park, T.G., Jeong, J.H., and Kim, S.W. (2006). Current status of polymeric gene delivery systems. Adv. Drug Deliv. Rev. *58*, 467–486.

27. Cao, H., Ouyang, H., Grasemann, H., Bartlett, C., Du, K., Duan, R., Shi, F., Estrada, M., Seigel, K.E., Coates, A.L., et al. (2018). Transducing airway basal cells with a helper-dependent adenoviral vector for lung gene therapy. Hum. Gene Ther. *29*, 643–652.

28. Palmer, D., and Ng, P. (2003). Improved system for helper-dependent adenoviral vector production. Mol. Ther. *8*, 846–852.

29. Cong, L., Ran, F.A., Cox, D., Lin, S., Barretto, R., Habib, N., Hsu, P.D., Wu, X., Jiang, W., Marraffini, L.A., and Zhang, F. (2013). Multiplex genome engineering using CRISPR/Cas systems. Science *339*, 819–823.

30. Ross, P.J., Kennedy, M.A., and Parks, R.J. (2009). Host cell detection of noncoding stuffer DNA contained in helper-dependent adenovirus vectors leads to epigenetic repression of transgene expression. J. Virol. *83*, 8409–8417.

31. Maruyama, T., Dougan, S.K., Truttmann, M.C., Bilate, A.M., Ingram, J.R., and Ploegh, H.L. (2015). Increasing the efficiency of precise genome editing with CRISPR-Cas9 by inhibition of nonhomologous end joining. Nat. Biotechnol. *33*, 538–542.

32. Chow, Y.H., Plumb, J., Wen, Y., Steer, B.M., Lu, Z., Buchwald, M., and Hu, J. (2000). Targeting transgene expression to airway epithelia and submucosal glands, prominent sites of human CFTR expression. Mol. Ther. *2*, 359–367.

33. Slaymaker, I.M., Gao, L., Zetsche, B., Scott, D.A., Yan, W.X., and Zhang, F. (2016). Rationally engineered Cas9 nucleases with improved specificity. Science *351*, 84–88.

34. Kleinstiver, B.P., Pattanayak, V., Prew, M.S., Tsai, S.Q., Nguyen, N.T., Zheng, Z., and Joung, J.K. (2016). High-fidelity CRISPR-Cas9 nucleases with no detectable genome-wide off-target effects. Nature *529*, 490–495.

35. Charlesworth, C.T., Deshpande, P.S., Dever, D.P., Dejene, B., Gomez-Ospina, N., Mantri, S., Pavel-Dinu, M., Camarena, J., Weinberg, K.I., and Porteus, M.H. (2018). Identification of pre-existing adaptive immunity to Cas9 proteins in humans. bioRxiv. https://doi.org/10.1101/243345.

36. Koehler, D.R., Sajjan, U., Chow, Y.-H., Martin, B., Kent, G., Tanswell, A.K., McKerlie, C., Forstner, J.F., and Hu, J. (2003). Protection of *Cftr* knockout mice from acute lung infection by a helper-dependent adenoviral vector expressing *Cftr* in airway epithelia. Proc. Natl. Acad. Sci. USA *100*, 15364–15369.

37. Sandig, V., Youil, R., Bett, A.J., Franlin, L.L., Oshima, M., Maione, D., Wang, F., Metzker, M.L., Savino, R., and Caskey, C.T. (2000). Optimization of the helper-dependent adenovirus system for production and potency in vivo. Proc. Natl. Acad. Sci. USA *97*, 1002–1007.

38. Lieber, M., Smith, B., Szakal, A., Nelson-Rees, W., and Todaro, G. (1976). A continuous tumor-cell line from a human lung carcinoma with properties of type II alveolar epithelial cells. Int. J. Cancer *17*, 62–70.

39. Zeitlin, P.L., Lu, L., Rhim, J., Cutting, G., Stetten, G., Kieffer, K.A., Craig, R., and Guggino, W.B. (1991). A cystic fibrosis bronchial epithelial cell line: immortalization by adeno-12-SV40 infection. Am. J. Respir. Cell Mol. Biol. *4*, 313–319.

40. Wu, Q., Chen, M., Buchwald, M., and Phillips, R.A. (1995). A simple, rapid method for isolation of high quality genomic DNA from animal tissues. Nucleic Acids Res. *23*, 5087–5088.